Experimental X-ray electron density study of atomic charges, oxidation states and inverted ligand field in $Cu(CF_3)_4^-$

Chen Gao,[1] Giovanni Macetti,[2] Vladimir Grushin,[3] Jacob Overgaard[1]*

[1] Department of Chemistry and Centre for Materials Crystallography, Aarhus University, Denmark.

[2] Dipartimento di Chimica, Università degli Studi di Milano, via C. Golgi 19, Milano 20133, Italy

[3] Central Research & Development, E. I. DuPont de Nemours & Co., Inc., Experimental Station, Wilmington, Delaware 19880, USA.

Electron density, topological analysis, inverted ligand field, oxidation state.

ABSTRACT The electron density distribution of the complex mono-anion $Cu(CF_3)_4$ has been studied by high-resolution X-ray single crystal diffraction and augmented with theoretical calculations. The study finds that the central copper bears an atomic charge of close to +1, while the occupancy of $d_{x^2-y^2}$ is only 1.26. Using a topological analysis and combined with theoretical analysis, the depopulation of $d_{x^2-y^2}$ is shown to be due to significant covalency in the Cu-C bonds.

The combination of the mono-valent picture and the covalency is interpreted as a confirmation of an inverted ligand field.

Introduction

The mono-anionic complex ion $[Cu(CF_3)_4]^-$ has recently been used as a test case for the investigation of the concept of oxidation states of metal ions and inverted ligand fields in coordination complexes. The history told here takes its beginnings with Snyder[1] reporting in 1995 that according to theoretical calculations, the five d-orbitals on Cu in $[Cu(CF_3)_4]^-$ are nearly completely filled, surprisingly also the central $d_{x^2-y^2}$-orbital, which is the energetically most disfavored one in this distorted square-planar ion, at least according to ligand field theory. This observation led Snyder to the controversial[2-3] claim that the oxidation state of the central Cu was +I, not +III, as was previously taken for granted. Snyder found support for this proposition by calculation of the NPA charge for Cu, which he found to be +0.71e at the MP2 level of theory. At first, such mono-valent description of Cu is difficult to reconcile with the presence of four equivalent ligands, as they can then no longer be identical. However, Snyder found an electronic population for the CF_3-group of 33.5e^-, which corresponds nicely to that of $CF_3^{-0.5}$, suggesting that we may more appropriately view the ligands as a whole as $(CF_3)_4^{2-}$, with three CF_3^{1-} and one CF_3^{1+}, rapidly interchanging such that the crystal structure shows four identical geometries.

Recently, an improved and much more straightforward synthesis of this ion was developed by Grushin *et al.*[4] Perhaps the improved access to this simple, yet electronically complex, compound provided the incentive for new investigations into the concept of inverted ligand fields. Obviously, theoretical possibilities have developed incredibly since the Snyder study in 1995, and recently

Lancaster[5] *et al.* combined new high level calculations with several advanced experimental techniques to show that the compound is best described as having an inverted ligand field and adopting a $3d^{10}4s^{0}$ electronic configuration. In particular, they used resonance inelastic x-ray scattering (RIXS) near the Cu K-edge to rule out the presence of a d^{8} ion. In their analysis, they accentuate the recent dismissal by Wieghardt *et al.*[6] of previous common conceptions that the observed pre-edge features are clear indicators for Cu(III).

Most recent is the quite philosophical contribution by Hoffmann *et al.*,[7] which was an important catalyst for the present experimental electron density study. Their work is devoted to several other systems than the one presented here, all falling under the umbrella of having potential inverted ligand fields. The authors put this question in a different context, while providing diverse and very relevant theoretical considerations.

Considering that the oxidation state of Cu and the associated valence electron count of the CF_3 ligands is strongly related to the electron density distribution (EDD), it is surprising that the latter has not seized a more prominent role in the many experimental and theoretical contributions. The fact is that the EDD is obtainable from accurate single crystal X-ray diffraction experiments[8] using a multipole model and it has been used in numerous studies to provide insight into the question of molecular reactivity, bonding analysis, aromaticity, etc.[9-12] The core of the approach is the fitting of population parameters related to atom-centered spherical harmonic function, as proposed by Hansen and Coppens,[13] and this advanced modeling requires data of the utmost quality.[8, 14-15]

Related to the question raised in this study there are two particularly important methods of analysis that deserves mentioning. *Firstly*, in 1990, Bader published his seminal book on the topic of Atoms In Molecules.[16] This theory has as its fundamental entity the concept of the atomic basins sub-dividing the physical space of a molecule into well-defined volumes containing one atom each,

and the electrons within the basin uniquely belong to that atom. This provides access to atomic volumes, and – thus – atomic charges by integration of the electron density within the volume. There exists alternative definitions of atomic charges in molecules,[17-18] since there is no unambiguous definition of atoms in molecules. However, as chemists seek simplification in order to reach usable insight, the atom as a notion when embedded in a molecule remains very much alive. This does not change the fact that the question of recovering oxidation states from ambiguous atomic charges is debatable. Certainly, charge decomposition methods often fail to recover the integral numbers used to represent formal oxidation states in chemistry textbooks, regardless of the scheme used.

The *second point* where a closer look at the EDD is sensible is the question of the occupation of the d-orbitals on Cu. The multipole model is constructed from atom-centered spherical harmonic functions, and there is a direct conversion of the refined population parameters to d-orbital populations.[19] The result is a list of d-orbital occupancies that would generate the EDD around the Cu-ion. This methodology has found application in diverse studies of magnetic properties and chemical bonding.[20-26] Critical is of course the occupancy of the $d_{x^2-y^2}$ orbital.

In addition to the experimental approaches, we implement two theoretical tools, the Delocalization Index (DI) and the Electron Localization Function (ELF). The DI is calculated from the integration of Fermi-hole density, and is essentially a measure of the number of shared electrons between two basins.[27-28] It is highly related with bond order, and can also be used to analyze weak interactions.[29] The features of chemical bonding can also be analyzed using the ELF,[30] defined as $\eta(r) = 1/[1 + \chi(r)^2]$. The kernel of ELF, χ(r), shows relatively the Pauli repulsion between two same-spin electrons. The higher χ(r) is, the higher Pauli repulsion there is, and thus the higher delocalization will be at that point. The ELF is scaled to range from 0 to 1, and

since $\chi(r)$ is in the denominator, it means high values of $\eta(r)$ represents high localization. Although ELF is only a relative measure of the electron localization, the basins of ELF show the space that electrons are localized in with respect to the homogeneous electron gas distribution, which refer to lone pairs, local bonds, etc.[31]

In this contribution, we have therefore collected high-resolution single crystal X-ray data on a specimen of $(Bu_4N)[Cu(CF_3)_4]$ (**1**), derived the experimental EDD and analyzed it using local and non-local tools, and compared these results to those obtained from theoretical calculations.

Experimental Section

Synthesis

Crystals of compound **1** were synthesized according to literature instructions.[4]

X-ray diffraction

A colorless, transparent single crystal was used in the experiment. Single crystal X-ray diffraction data were collected on an Oxford Diffraction Supernova diffractometer equipped with an Atlas CCD detector and MoKα-radiation at Aarhus University. The crystal was cooled to a temperature of 100(1) K using an Oxford Cryosystems Cryostream 700. The maximum achievable resolution was limited ($\sin\theta/\lambda < 0.93$ Å^{-1}) due to the thermal motion of the large cations in the crystal structure. Within that resolution range, a complete data set with an average redundancy of 8.6 was collected. The data was integrated using CrysalisPro (version 39.46) and frame scale factors as well as absorption correction were applied using SCALEPACK. The integrated intensities were merged in the Laue group 2/m using SORTAV.[32-33] A correction for low energy contamination is applied to all (3h3k3l) reflections, which led to a significant improvement of the fit.[34-35] The structure was solved by direct methods encoded in SHELXT[36] and an independent atom model (IAM) refinement was performed with SHELXL[37] in Olex2[38] to obtain the molecular

structure. Relevant crystallographic information is listed in Table 1, and an ORTEP drawing shown in Figure 1.

Table 1 Crystallographic details for **1**

	1
Formula	$CuC_{20}H_{36}F_{12}N$
Molecular Mass	582.04
Crystal size (μm)	255×130×110
Temperature (K)	100(1)
Crystal system	Monoclinic
Space group	$P2_1/n$
a (Å)	9.15435(15)
b (Å)	16.8820(3)
c (Å)	17.3303(3)
α (°)	90
β (°)	99.2229(15)
γ (°)	90
Volume ($Å^3$)	2643.67(8)
Z	4
No. of reflections collected	158980
No. unique	18577
R_{int}	0.0481
Completeness (%)	99.97
No. reflections used	14127
ρ_c (gcm^{-1})	1.462
F(000)	1200

μ (mm^{-1})	0.92
$\sin \theta/\lambda_{max}$	0.93
θ range for data collection (°)	2.381-42.105
	-17<h<17
Index ranges	-31<k<31
	-32<l<32
IAM Refinement	
Final R(F), wR2(F2)	0.0403, 0.0926
Goodness of fit	1.069
Max/min residual density ($eÅ^{-3}$)	0.58, -0.50
Multipole Refinement	
N_{obs}/N_{var}	15.995
R(F), $R(F^2) > 2\sigma(F)$	0.0290, 0.0289
R(F), $R(F^2)$, all data	0.0492, 0.0329
$R_w(F)$, $R_w(F^2) > 2\sigma(F)$	0.0216, 0.0403
Goodness of fit	1.6942
Max/min residual density ($eÅ^{-3}$)	0.41, -0.39

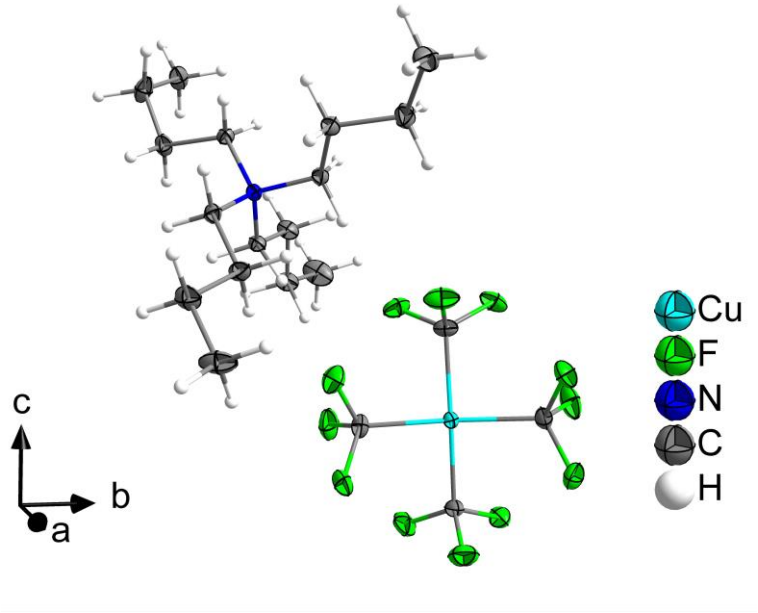

Figure 1. ORTEP[39] drawing of **1** shown with 50% probability ellipsoids.

Multipole Modeling

Aspherical electron density features were modeled based on the Hansen-Coppens multipole formalism[13] using the XD2016 package.[40] Radial functions of core and valence were taken from the accompanying bank file, which is based on Clementi and Roetti's results. The structure from IAM refinement is used as input for XD2016. The general procedure adhered to in the refinement was: initially, the positions and anisotropic displacement parameters (ADPs) of non-hydrogen atoms were refined based on high angle reflections ($\sin\theta/\lambda > 0.6$ Å^{-1}). Secondly, the parameters refined in the first step are fixed, positions and isotropic displacement parameters of hydrogen atoms are refined based on low angle reflections ($\sin\theta/\lambda < 0.6$ Å^{-1}). After the refinement, the C-H bond lengths are reset according to tabulated neutron diffraction literature values.[41] Anisotropic thermal parameters for the hydrogen atoms were then calculated using SHADE3.[42] After the refinement of the structural parameters, multipole parameters are included gradually. κ and P_v for all the atoms was refined with the constraint that the crystal structure remained charge neutral. The

charge of the different ions, $Cu(CF_3)_4^-$ and $(^nBu)_4N^+$, are constrained to -1 and +1, respectively. For all atoms, κ and κ′ parameters are constrained to be the same. Independent κ-parameters were defined for carbon atoms based on the chemical environment in the molecule, which means that all carbon atoms are categorized as belonging to either a CF_3 group (coordinating atoms), a CH_2 group or a CH_3. Higher order population parameters were then gradually included in the refinement. Neutral scattering factors were applied for all atoms except for Cu. For the radial function of the valence shell of Cu, we tested both $3d^{10}4s^0$ and $3d^{10}4s^1$. In order to limit the number of employed parameter, we introduced symmetry constraints on some of the atoms: all CH_2 carbons are constrained to exhibit C_{2v} symmetry and CH_3 to C_{3v} symmetry. All alkane chains on the counter ion, except for the C13-C16 chain, were constrained to be the same. For the hydrogens, only dipoles in the bond direction are used. The κ- and κ′-parameters of hydrogen atoms are fixed to a value of 1.2. Crystallographic output and a detailed evaluation of the fit[14] is given in the SI (fig. S1 – S4).

Computational Details

Density functional theory (DFT) calculation of the anion $Cu(CF_3)_4^-$ was performed in ORCA 4.0.1 software package.[43] Single point energy was calculated based on crystallographic coordinates after the multipole refinement from single crystal X-ray diffraction. Hybrid functionals B3LYP were used in the calculation. ZORA-def2-TZVP basis set was used for all the atoms, while scalar relativistic effect ZORA calculation was also performed. RIJCOSX approximation was applied to speed up the calculation of coulomb integral and Hartree-Fock exchange, with the help of auxiliary basis set SARC/J. QTAIM analysis, ELF calculation and analysis based DFT wavefunctions were performed using Multiwfn software.[44] All basin integrations (electron population and source function in AIM basins, electron population in ELF basins) are done with a mesh size of 0.04 bohr.

Results and Discussion

The four CF_3 ligands form a pseudo square-planar coordination geometry around Cu, with a mean deviation of C-atoms of 0.235(2) Å from the least squares CuC_4-plane. Generally, a four-coordinate ion with a d^{10} electron configuration should exhibit tetrahedral and not square planar geometry, but previous results have shown that in the presence of an inverted ligand field,[5, 7] it will result in unfilled ligand σ orbitals, whose splitting cause the square-planar geometry to be energetically favored.

Atomic charges and d-orbital populations

According to Snyder (Figure 2, remade from Figure 1 in reference 1), the four ligand orbitals based primarily on the carbon atoms of the $CF_3^{0.5-}$ ligands pointing towards Cu combine to give four molecular orbitals, of which two are symmetric and the other two are anti-symmetric.

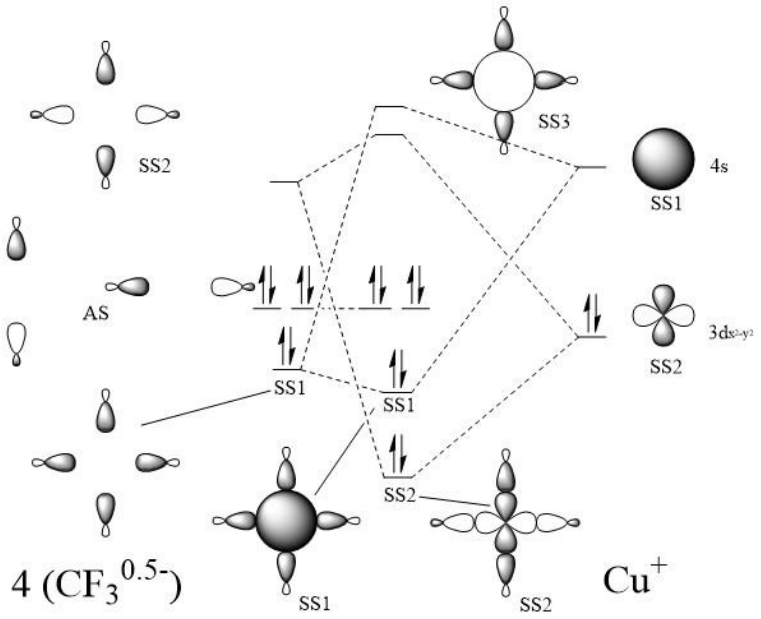

Figure 2. Idealized MO correlation diagram for the Cu-C bonding. Adapted from reference [1].

The symmetric orbital, SS2, with the same symmetry as $d_{x^2-y^2}$ on Cu has the highest energy and is thus empty in the configuration shown if Figure 2. The interaction of $d_{x^2-y^2}$ with SS2

results in a transfer of electrons from the metal to the ligand, while electrons are back-donated from the fully occupied and symmetrical SS1 to the empty 4s. Because the ligand molecular orbitals are linear combinations of the four ligand σ-orbitals, the result of these considerations is a depletion of $d_{x^2-y^2}$, the possibility for non-zero population in the formally empty 4s and SS2 orbitals.

In order to experimentally examine the presence of 4s population, we attempted a separate description of the 4s electrons. This is particularly difficult, as these are rather diffuse in space and with low population, equivalent to a quite small additional spherical component of electron density in the valence region. As mentioned in the experimental section, we refined models with and without 4s electrons, and they are equally good with slightly larger residuals when 4s is included, and the final model used below is therefore not including 4s electrons.

Contrary to the problematic determination of 4s electrons, it is much less complicated to examine the population in the $d_{x^2-y^2}$ orbital. Qualitatively, the static deformation density map (Figure 3) indicates clearly that this orbital is less populated than the expected two electrons it holds in a neutral, isolated Cu-atom having a $3d^{10}$ configuration. Quantitatively, the refined multipoles can be converted into d orbital population using a simple transformation.[19] The result (see Table 2) is very clearly four fully occupied orbitals and then $d_{x^2-y^2}$ which is only slightly more than singly occupied.

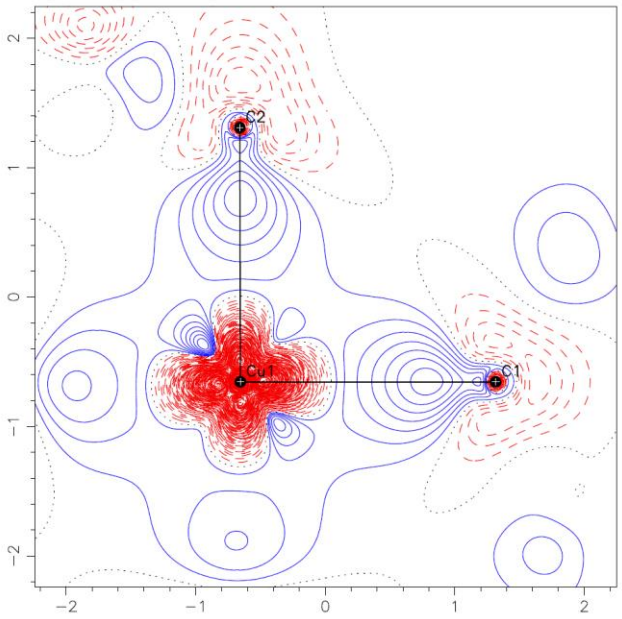

Figure 3. Deformation density map of $Cu(CF_3)_4^-$ in the C(1)-Cu(1)-C(2) plane. Positive (blue line) and negative (red dash) contours are shown at intervals of 0.1eÅ^{-3}.

Table 2. 3d orbital population of Cu in $Cu(CF_3)_4^-$. The local coordinate systems is defined by the midpoint C(1) and C(3)

orbital	population	percentage
d_{z^2}	2.29	23.3%
d_{xz}	2.06	21.0%
d_{yz}	2.20	22.4%
$d_{x^2-y^2}$	1.26	12.8%
d_{xy}	2.01	20.4%
Total d population	9.82	100

In contrast to d-orbitals, it is not possible to extract the population of the SS2 molecular orbital directly from the multipole model. In order to answer that we need to resort to another spatial decomposition scheme, namely the ELF (*vide infra*). However, before resuming the analysis of the SS2 population, we use the EDD to examine the question of oxidation state for Cu. Table 3 shows the atomic and group charges that result from integration according to QTAIM space partitioning. Conspicuously, the integrated charge of Cu (+1.03) supports its classification as Cu(I), as we observe a valence shell configuration of $3d^{9.82}$ (see Table 3) instead of $3d^{8}$ expected for the Cu(III)-ion. As mentioned above, it is possible that there is a small population in the 4s-orbital that we cannot determine experimentally due to its diffuse and isotropic nature. The experimental AIM charges are similar to those found from the theoretical wavefunction, and both convey a picture of Cu(I) surrounded by four $(CF_3)^{0.5-}$ ligands. The total valence shell population (9.82(3), see Table 2) as obtained from the refined monopole parameter gives Cu a charge of +1.18(3) which is in complete accord with the AIM charges.

Table 3. AIM charges of $Cu(CF_3)_4^-$

	Experiment	**Theory**
$\langle q_\Omega \rangle, C$	+2.06(6)	+1.44
$\langle q_\Omega \rangle, F$	–0.86(4)	–0.64
$4 * \langle q_\Omega \rangle, CF_3$	–2.08(5)	–1.88
q_Ω, Cu	+1.03	+0.87
$\sum q_{\Omega,\mathrm{anion}}$	–1.04	–1.00

Chemical bonding in the $Cu(CF_3)_4$-anion

In order to estimate the population of the SS2 orbital, we combine the AIM analysis with the ELF. Figure 4 shows the ELF in the C(1)-Cu(1)-C(2) plane. From a topological analysis using the gradient of the ELF, separate basins can be distinguished and their electronic populations integrated (see Table 5). Specifically, we locate four disynaptic basins, each with an electronic population of 2.04, on the bond paths of the Cu-C bonds near the C-atoms. The AIM bond critical points of the Cu-C bonds lie within these ELF basins, meaning that a fraction of the valence electrons of Cu are located inside these ELF bond basins. To estimate the size of this fraction, we can use the Raub-Jansen Index (RJI), which uses the contribution from different AIM basins to the ELF bond basins to estimate the bond polarity.[45] Atoms with large electronegativity have larger contributions to the ELF bond basin electron populations, meaning that most of the ELF bond basins belong to the AIM atomic basin of the electronegative atom.[46] For a non-polar homo-nuclear covalent bond, RJI is 50%, while for a classical dative bond RJI is above 95%.[47-48] In the case of **1**, the RJI is only 81%, clearly showing an increased electron sharing between Cu and its ligands, relative to that of a dative bond. If we divide the electronic population of 2.04 of the ELF bond basin into atomic parts based on the RIJ, we obtain 1.65 electrons on carbon. In addition, about 0.04 electrons belong to the fluorine atoms, the basins of which also penetrate the ELF Cu-C bond basin. In total, this gives 1.4 electrons that can be ascribed to Cu, meaning that 0.6 electrons are transferred from a filled $d_{x^2-y^2}$ orbital to the SS2 orbital, and which matches very well with the experimentally determined d-orbital population of 1.26.

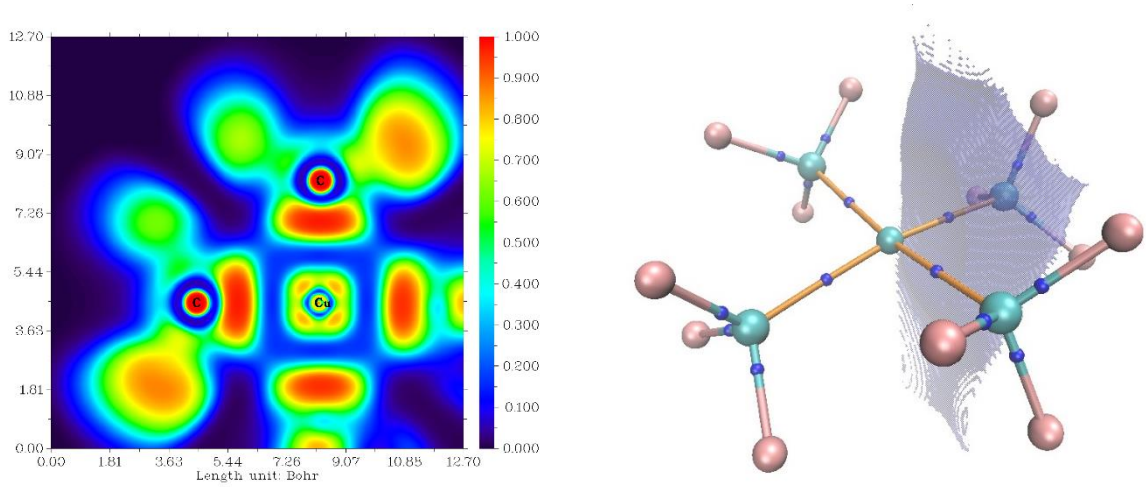

Figure 4. Left: ELF map on C(1)-Cu-C(2) plane. Right: ELF Basin border of the coordination bond Cu-C(1), note that the bcp is inside the basin.

Table 5. ELF basin electron populations.

	Average populations
Cu valence lone pairs	4.08(7)
Cu-C bonds	2.04
Cu Core	10.43

As a final note, let us take a look at the extent of direct interaction between the ligands, which is relevant in the context of Figure 2, where we view the bonding between the central Cu and the four combined σ-orbitals of the ligands. This may be quantified by an evaluation of the DI.[49] The DIs between neighboring carbon atoms (given as δ(C,C)) are low (0.057 for neighbors and 0.047 for opposite carbons), meaning that only 0.057/0.047 electron pairs are shared between the corresponding AIM basins. It may be more appropriate to look at the DI between fluorine atoms in one ligand and the carbon in its neighboring ligand: δ(F,C) is 0.0214, which is smaller but

comparable to δ(C,C). Summing up all inter-ligand DIs gives values of 0.204 and 0.111 for the neighboring and opposite groups, respectively.

In order to evaluate the delocalization among ligands in more detail, we carried out a calculation with the central Cu(I) removed. In the resulting wavefunction for this model (**1a**), we find four molecular orbitals created by the lone pairs on the four C-atoms. Among these four orbitals (Figure S5), the one having the same symmetry as a Cu $d_{x^2-y^2}$ (similar to SS2) is completely empty. For this hypothetical molecule, we find δ(C,C)-values of 0.17 (neighbor) and 0.13 (opposite), which suggests that the bonding in this tetrameric anion enables the sharing of electrons through space. If we add two electrons to the system this gives us (**1b**), corresponding to the case where we remove a Cu(III), we find that all four σ-type molecular orbitals are fully occupied, and δ(C,C)-values decrease to 0.10 (neighbor) and 0.015 (opposite). Thus, by adding two electrons the electron sharing between carbons decreases, especially for the opposite carbons. The reason for this is that the HOMO in **1b** is the anti-bonding version of the HOMO-4 in **1** (see Figure 2). If we compare δ(C,C) between neighboring ligands relative to that between opposite ligands, it is conspicuous that these are rather similar in **1** and **1a**, while highly different in **1b**. We may interpret this as supporting the view of **1** as being Cu(I).

Table 4. Selected delocalization indices of $Cu(CF_3)_4^-$

	$Cu(CF_3)_4^-$	**$4(CF_3)^{0.5-}$**	**$4(CF_3)^{1-}$**
δ(F,C) (different ligands)	0.0214	0.0437	0.243
δ(C,C)(neighbor)	0.057	0.17	0.10
δ(C,C)(opposite)	0.047	0.13	0.015
δ(F,C) (same ligand)	0. 705	0.745	0.747
δ(Cu,C)	0. 646	--	--

Conclusions

We have collected high resolution, high redundancy single crystal X-ray diffraction data of the compound $(Bu_4N)[Cu(CF_3)_4]$ and used multipole modeling to study the electron density distribution. Using Bader's decomposition of Atoms In Molecules, we find an electron population on Cu by integration of the basin corresponding to an atomic charge close to +1. This is corroborated by the total electron count of the d-orbitals, which is near 9.8. The experimentally derived occupancy of the important $d_{x^2-y^2}$ orbital is 1.26. This value compares very well with the expected orbital occupancy after transfer to the SS2 molecular orbital formed by the ligand σ-orbitals, as obtained by a Raub-Jansen Index decomposition of the ELF-based bond basin into atomic components. The Raub-Jansen index shows a significant decrease in bond polarity compared to common coordination bonds, suggesting some extent of covalency. This is supported by the topological analysis of the electron density, which provides clearly negative energy densities at the Cu-C bond critical points as a sign of strong covalent contributions. The behavior of the charge distributions in this anion supports the existence of an inverted ligand field, leading to large electronic population on Cu.

ASSOCIATED CONTENT

The following files are available free of charge.

brief description (file type, i.e., PDF)

brief description (file type, i.e., PDF)

AUTHOR INFORMATION

Corresponding Author: jacobo@chem.au.dk

Author Contributions

The manuscript was written through contributions of all authors. All authors have given approval to the final version of the manuscript.

Funding Sources

Danish National Research Foundation (DNRF-93).

ACKNOWLEDGMENT

The authors would like to thank the Danish National Research Foundation for funding for the project (DNRF-93).

ABBREVIATIONS

REFERENCES

1. Snyder, J. P., Elusiveness of CuIII Complexation; Preference for Trifluoromethyl Oxidation in the Formation of [CuI(CF3)4]− Salts. *Angew. Chem. Int. Ed. Engl.* **1995,** *34* (1), 80-81.
2. Snyder, J. P., Distinguishing Copper d8 and d10 Configurations in a Highly Ionic Complex; A Nonformal Metal Oxidation State. *Angew. Chem. Int. Ed. Engl.* **1995,** *34* (9), 986-987.
3. Kaupp, M.; von Schnering, H. G., Formal Oxidation State versus Partial Charge—A Comment. *Angew. Chem. Int. Ed.* **1995,** *34* (9), 986-986.
4. Romine, A. M.; Nebra, N.; Konovalov, A. I.; Martin, E.; Benet-Buchholz, J.; Grushin, V. V., Easy Access to the Copper(III) Anion [Cu(CF3)4]−. *Angew. Chem. Int. Ed.* **2015,** *54* (9), 2745-2749.
5. Walroth, R. C.; Lukens, J. T.; MacMillan, S. N.; Finkelstein, K. D.; Lancaster, K. M., Spectroscopic Evidence for a 3d10 Ground State Electronic Configuration and Ligand Field Inversion in [Cu(CF3)4]1−. *J. Am. Chem. Soc.* **2016,** *138* (6), 1922-1931.
6. Tomson, N. C.; Williams, K. D.; Dai, X.; Sproules, S.; DeBeer, S.; Warren, T. H.; Wieghardt, K., Re-evaluating the Cu K pre-edge XAS transition in complexes with covalent metal–ligand interactions. *Chem. Sci.* **2015,** *6* (4), 2474-2487.

7. Hoffmann, R.; Alvarez, S.; Mealli, C.; Falceto, A.; Cahill, T. J.; Zeng, T.; Manca, G., From Widely Accepted Concepts in Coordination Chemistry to Inverted Ligand Fields. *Chem. Rev.* **2016,** *116* (14), 8173-8192.
8. Coppens, P., *X-Ray Charge Densities and Chemical Bonding (IUCr Texts on Crystallography)*. IUCr: 1997; p 384.
9. Stalke, D., Charge Density and Chemical Bonding. In *The Chemical Bond I: 100 Years Old and Getting Stronger*, Mingos, D. M. P., Ed. Springer International Publishing: Cham, 2016; pp 57-88.
10. Overgaard, J.; Iversen, B. B., Charge Density Methods in Hydrogen Bond Studies. In *Electron Density and Chemical Bonding I*, Stalke, D., Ed. Springer Berlin Heidelberg: 2012; pp 53-74.
11. Schmokel, M. S.; Cenedese, S.; Overgaard, J.; Jorgensen, M. R. V.; Chen, Y. S.; Gatti, C.; Stalke, D.; Iversen, B. B., Testing the Concept of Hypervalency: Charge Density Analysis of K2SO4. *Inorg. Chem.* **2012,** *51* (15), 8607-8616.
12. Stalke, D., Meaningful Structural Descriptors from Charge Density. *Chemistry-a European Journal* **2011,** *17* (34), 9264-9278.
13. Hansen, N. K.; Coppens, P., Electron Population Analysis of Accurate Diffraction Data .6. Testing Aspherical Atom Refinements on Small-Molecule Data Sets. *Acta Crystallogr. Sect. A* **1978,** *34* (Nov), 909-921.
14. Herbst-Irmer, R.; Stalke, D., Experimental charge-density studies: data reduction and model quality: the more the better? *Acta Crystallogr. Sect. B* **2017,** *73* (4), 531-543.
15. Wolf, H.; Jorgensen, M. R. V.; Chen, Y.-S.; Herbst-Irmer, R.; Stalke, D., Charge density investigations on [2,2]-paracyclophane - in data we trust. *Acta Crystallogr. Sect. B* **2015,** *71* (1), 10-19.
16. Bader, R. F. W., *Atoms in Molecules : A Quantum Theory*. Clarendon Press: Oxford, 1990; p xviii, 438 p.
17. Bultinck, P.; Alsenoy, C. V.; Ayers, P. W.; Carbó-Dorca, R., Critical analysis and extension of the Hirshfeld atoms in molecules. *J. Chem. Phys.* **2007,** *126* (14), 144111.
18. Reed, A. E.; Weinstock, R. B.; Weinhold, F., Natural population analysis. *J. Chem. Phys.* **1985,** *83* (2), 735-746.
19. Holladay, A.; Leung, P.; Coppens, P., Generalized Relations between D-Orbital Occupancies of Transition-Metal Atoms and Electron-Density Multipole Population Parameters from X-Ray-Diffraction Data. *Acta Crystallogr. Sect. A* **1983,** *39* (May), 377-387.
20. Craven, M.; Nygaard, M. H.; Zadrozny, J. M.; Long, J. R.; Overgaard, J., Determination of d-Orbital Populations in a Cobalt(II) Single-Molecule Magnet Using Single-Crystal X-ray Diffraction. *Inorg. Chem.* **2018,** *57* (12), 6913-6920.
21. Sohtome, Y.; Nakamura, G.; Muranaka, A.; Hashizume, D.; Lectard, S.; Tsuchimoto, T.; Uchiyama, M.; Sodeoka, M., Naked d-orbital in a centrochiral Ni(II) complex as a catalyst for asymmetric [3+2] cycloaddition. *Nat. Commun.* **2017,** *8*, 14875.
22. Schmokel, M. S.; Bjerg, L.; Cenedese, S.; Jorgensen, M. R. V.; Chen, Y.-S.; Overgaard, J.; Iversen, B. B., Atomic properties and chemical bonding in the pyrite and marcasite polymorphs of FeS2: a combined experimental and theoretical electron density study. *Chem. Sci.* **2014,** *5*, 1408-1421.
23. Deutsch, M.; Claiser, N.; Gillet, J. M.; Lecomte, C.; Sakiyama, H.; Tone, K.; Souhassou, M., d-Orbital orientation in a dimer cobalt complex: link to magnetic properties? *Acta Crystallogr. Sect. B-Struct. Sci.* **2011,** *67*, 324-332.

24. Overgaard, J.; Larsen, F. K.; Timco, G. A.; Iversen, B. B., Experimental charge density in an oxidized trinuclear iron complex using 15 K synchrotron and 100 K conventional single-crystal X-ray diffraction. *Dalton Trans.* **2009,** (4), 664-671.
25. Bunting, P. C.; Atanasov, M.; Damgaard-Møller, E.; Perfetti, M.; Crassee, I.; Orlita, M.; Overgaard, J.; Van Slageren, J.; Neese, F.; Long, J. R., A Linear Cobalt(II) Dialkyl Complex with Maximal Orbital Angular Momentum Arising from a non-Aufbau Ground State. *Science* **2018,** *in press*.
26. Thomsen, M. K.; Nyvang, A.; Walsh, J. P. S.; Bunting, P. C.; Long, J. R.; Neese, F.; Atanasov, M.; Genoni, A.; Overgaard, J., Insights into single-molecule magnet behavior from the experimental electron density of linear two-coordinate iron complexes. *Angew. Chem. Int. Ed. Engl.* **2018,** *submitted*.
27. Firme, C. L.; Antunes, O. A. C.; Esteves, P. M., Relation between bond order and delocalization index of QTAIM. *Chem. Phys. Lett.* **2009,** *468* (4–6), 129-133.
28. Bader, R. F. W.; Streitwieser, A.; Neuhaus, A.; Laidig, K. E.; Speers, P., Electron delocalization and the Fermi hole. *J Am Chem Soc* **1996,** *118* (21), 4959-4965.
29. Hugas, D.; Guillaumes, L.; Duran, M.; Simon, S., Delocalization indices for non-covalent interaction: Hydrogen and DiHydrogen bond. *Computational and Theoretical Chemistry* **2012,** *998*, 113-119.
30. Becke, A. D.; Edgecombe, K. E., A Simple Measure of Electron Localization in Atomic and Molecular-Systems. *J. Chem. Phys.* **1990,** *92* (9), 5397-5403.
31. Chamorro, E.; Fuentealba, P.; Savin, A., Electron probability distribution in AIM and ELF basins. *J Comput Chem* **2003,** *24* (4), 496-504.
32. Blessing, R. H., An empirical correction for absorption anisotropy. *Acta crystallographica. Section A, Foundations of crystallography* **1995,** *51 (Pt 1)*, 33-8.
33. Blessing, R. H.; Langs, D. A., Data averaging with normal down-weighting of outliers. *J. Appl. Crystallogr.* **1987,** *20* (5), 427-428.
34. Krause, L.; Herbst-Irmer, R.; Stalke, D., An empirical correction for the influence of low-energy contamination. *J. Appl. Crystallogr.* **2015,** *48* (6), 1907-1913.
35. Macchi, P.; Burgi, H.-B.; Chimpri, A. S.; Hauser, J.; Gal, Z., Low-energy contamination of Mo microsource X-ray radiation: analysis and solution of the problem. *J. Appl. Crystallogr.* **2011,** *44* (4), 763-771.
36. Sheldrick, G., SHELXT - Integrated space-group and crystal-structure determination. *Acta Crystallogr. Sect. A* **2015,** *71* (1), 3-8.
37. Sheldrick, G., Crystal structure refinement with SHELXL. *Acta Crystallogr. Sect. C* **2015,** *71* (1), 3-8.
38. Dolomanov, O. V.; Bourhis, L. J.; Gildea, R. J.; Howard, J. A. K.; Puschmann, H., OLEX2: a complete structure solution, refinement and analysis program. *J. Appl. Crystallogr.* **2009,** *42*, 339-341.
39. Johnson, C. K. *ORTEP*, Oak Ridge National Laboratory, Tennessee, USA: 1965.
40. Volkov, A.; Macchi, P.; Farrugia, L. J.; Gatti, C.; Mallinson, P. R.; Richter, T.; Koritsanszky, T. *XD2006 - a computer program for multipole refinement, topological analysis and evaluation of intermolecular energies from experimental and theoretical structure factors.*, revision 5.34; University at Buffalo, State University of New York, Buffalo, NY, University of Milano, Milano, Italy, University of Glasgow, Glasgow, U.K., CNRISTM, Milano, Italy, and Middle Tennessee State University Murfreesboro, TN, 2006.

41. Allen, F. H.; Kennard, O.; Watson, D. G.; Brammer, L.; Orpen, A. G.; Taylor, R., Tables of bond lengths determined by X-ray and neutron diffraction. Part 1. Bond lengths in organic compounds. *Journal of the Chemical Society, Perkin Transactions 2* **1987,** (12), S1-S19.
42. Madsen, A. O.; Hoser, A. A., SHADE3 server: a streamlined approach to estimate H-atom anisotropic displacement parameters using periodic ab initio calculations or experimental information. *J. Appl. Crystallogr.* **2014,** *47* (6), 2100-2104.
43. Neese, F., Software update: the ORCA program system, version 4.0. *Wiley Interdisciplinary Reviews: Computational Molecular Science* **2018,** *8* (1), e1327.
44. Lu, T.; Chen, F., Multiwfn: A multifunctional wavefunction analyzer. *Journal of Computational Chemistry* **2012,** *33* (5), 580-592.
45. The Raub-Jansen index is in fact based on the intersection of AIM and ELI-D basins. However, we have applied it here as the ELF and ELI-D basins are virtually identical.
46. Raub, S.; Jansen, G., A quantitative measure of bond polarity from the electron localization function and the theory of atoms in molecules. *Theor Chem Acc* **2001,** *106* (3), 223-232.
47. Beckmann, J.; Heinrich, D.; Mebs, S., Molecular Structure and Real-Space Bonding Descriptors (AIM, ELI-D) of Phenyl(triphenylstannyl)telluride. *Z Anorg Allg Chem* **2013,** *639* (12-13), 2129-2133.
48. Mebs, S.; Grabowsky, S.; Förster, D.; Kickbusch, R.; Hartl, M.; Daemen, L. L.; Morgenroth, W.; Luger, P.; Paulus, B.; Lentz, D., Charge Transfer via the Dative N−B Bond and Dihydrogen Contacts. Experimental and Theoretical Electron Density Studies of Small Lewis Acid−Base Adducts. *The Journal of Physical Chemistry A* **2010,** *114* (37), 10185-10196.
49. Fradera, X.; Austen, M. A.; Bader, R. F. W., The Lewis model and beyond. *J. Phys. Chem. A* **1999,** *103* (2), 304-314.